

Growth of aligned arrays of ZnO nanorods by low temperature solution method on Si surface

R. CHANDER

Materials Research Center, Indian Institute of Science, Bangalore-560012, India

A. K. RAYCHAUDHURI*

*Materials Research Center, Indian Institute of Science, Bangalore-560012, India; Department of Physics, Indian Institute of Science, Bangalore-560012, India; Unit for Nanoscience and Technology, S.N. Bose National Center for Basic Sciences, Kolkata-700 098, India
E-mail: arup@bose.res.in*

Published online: 21 April 2006

We report growth of ZnO nanorods by low temperature ($<100^{\circ}\text{C}$) solution growth method. The substrates (Si, glass and fused Quartz) were seeded by pre-coating with ZnO nanoparticles (4–7 nm diameter) prepared by chemical precipitation route. Nanorods were grown on the seeded substrate in aqueous solution of Zinc Nitrate and Hexamethylenetetramine (HMT). The growth process lasts for up to 8 h and at the maximum time of growth, the nanorods have a width of $\sim 230\text{--}250$ nm and length of $\sim 1.5\text{--}1.6$ μm . The growth process after some initial growth (<2 h) preserves the aspect ratio and leads to about 90% texturing along the (002) direction. The growth of the nanorods was studied with time and observed growth data suggests a two-stage growth process. The nanorods have a well-defined hexagonal morphology and have a Wurtzite structure. The nanorods were characterized by different techniques and have a band gap of 3.25 eV. © 2006 Springer Science + Business Media, Inc.

1. Introduction

ZnO is one of the widely studied materials for its number of exciting properties. It is a wide band gap semiconductor material with $E_g \approx 3.3$ eV. ZnO has large excitonic binding energy of ~ 60 meV [1]. This property makes it a very useful material for room temperature UV lasing application [2]. It is used for gas sensing applications [3], surface acoustic wave devices [4], transparent coating and solar cell applications [5]. In recent years there has been intense activity to grow ZnO nanorods using a number of techniques like vapor phase transport technique [6], thermal decomposition of precursors [7, 8], oxidation of Zn metal [9] or reduction followed by oxidation of ZnS powder [10] at high temperature and inert environment. Catalytic growth of zinc oxide nanowires by vapor transport has been widely used in the past for making ZnO based devices [6]. Seed controlled vapor phase growth method has been used to make arrays of needles of aligned ZnO [11]. There are reports of well-aligned ZnO nanowires made by metallo-organic vapor-phase growth method [12]. There are reports of catalyst free synthesis of nanowire arrays on Si [13]. These techniques involve

high processing temperatures [6, 8, 10–12]. Some of these vapor phase techniques also do not provide high degree of alignment and special growth conditions are required and therefore cannot be used for many of the device applications. An important issue in vapor phase growth is the quality of the substrate. Often, costly substrates like Al_2O_3 is required for oriented growth from vapor phase. A non-vapor phase method is the use of electrodeposition of metallic Zn in nanoporous membranes followed by thermal oxidation [14]. Thus we note that most of the reported methods involve high to moderately high temperature processes to synthesize ZnO nanowires/rods. For a technique to be viable for commercial applications it is desirable that the growth temperature should be made low enough to make it energy efficient. Recently there have been successful attempts to grow the ZnO nanorods by solution method [15–17]. This method brings the growth temperature down to below 100°C . Aligned nanorods of ZnO were grown on F-SnO₂ or ITO coated substrates (without nanoparticle seeding) using zinc nitrate tetrahydrate and methenamine [15]. The rods were aligned along [001] and had diameters in the range of 1 μm . Nanorods

*Author to whom all correspondence should be addressed.

of ZnO were grown on glass substrates by pre-seeding them with ZnO nanocrystals by dip coating [16]. The seed nanocrystals were in the size range 24–71 nm. The rods were grown from zinc nitrate tetrahydrate and hexamethyltetramine and the morphology was controlled by adding citrate ions. The diameter of the grown rods was in the range of 250 nm. Such methods can be used for large area coating as demonstrated by growing aligned rods on a 10 cm Si wafer [17]. The diameters achieved are in the range of 200–300 nm. Prior seeding of the surface by ZnO nanocrystals leads to nucleation sites on which ZnO nanorods can grow in a highly aligned fashion. It is interesting that aligned growth depends mainly on prior seeding and this makes it essentially independent of the morphology of the substrate used.

In this paper we report the low temperature ($<100^{\circ}\text{C}$) synthesis of vertically aligned arrays of ZnO nanorods (with Wurtzite structure) similar to that given in references [15–17] and report the study of the growth process and the growth kinetics, in particular, by using Scanning Probe Microscopy (SPM) and Scanning Electron Microscopy (SEM). The synthesis of aligned compact arrays of ZnO nanorods was done by a simple solution technique on a surface that has been pre-seeded with ZnO nanoparticles of size $\sim 4\text{--}7$ nm. This size of seed nanoparticles is much smaller compared to that used in the past [16]. We have also seeded the substrate with a larger density of nanoparticles ($\sim 10^{11}\text{--}10^{12}/\text{cm}^2$). This along with a close control on the growth condition made us achieve better orientation ($\sim 90\%$) compared to past studies (40–50%). We describe in detail below the synthesis method that gives rise to such aligned growth. This work is a continuation of the technique reported in ref. [17]. However, we use smaller seed particles, larger seed density and address several new issues related to the growth, namely, the nature and necessity of the seeded surface, growth of texture and aspect ratio as a function of time and use Lateral Force Microscopy to study the roughness of the nanorods.

2. Experimental details

A two-step process has been used to grow ZnO nanorods by low temperature solution growth method. The first step is the seeding of the substrate by the ZnO nanoparticles. The second step consists of using the nanoparticles seeded substrate for further growth of the nanorods. The following subsections describe the processes.

2.1. Seeding the substrate

In the first step ZnO nanoparticles with size in the range 4–7 nm were synthesized by slowly adding 0.03 M NaOH solution in methanol to 0.01 M solution of $\text{Zn}(\text{CH}_3\text{COO})_2 \cdot 2\text{H}_2\text{O}$ in methanol kept at 60°C [18]. The final solution was stirred and heated at 60°C for 1h prior to seeding. Commercially available ZnO nanoparticles can also be used as has been done in the past [16]. However, the sizes of the available particles have much larger aver-

age size (>25 nm) as well as a much larger spread in size (20–70 nm).

The growth was carried on p-type silicon with resistivity $10\ \Omega\text{-cm}$, borosilicate glass and fused Quartz substrates coated with ZnO nanoparticles. Similar results have been obtained on all the substrates used. In this paper we only describe the data taken on Si substrate to avoid repetition. These nanoparticles act as nucleating sites leading to aligned growth of nanorods. Prior to seeding by nanoparticles, the substrates were cleaned ultrasonically with organic solvents acetone, methanol and chloroform and then cleaned with a solution of $\text{H}_2\text{SO}_4\text{:H}_2\text{O}_2$ having 2:1 ratio. Cleaned substrates were coated with ZnO nanoparticles by spin coating at a speed of around 3000–3500 r.p.m. Two drops of nanoparticles colloidal solution were used for each substrate. The coated substrates were heated at 125°C for 1h for the better adherence of nanoparticles.

2.2. Solution growth of nanorods

The next step of the process is to grow nanorods onto these seeded surfaces by an aqueous route. Aqueous solution of (0.03 M) $\text{Zn}(\text{NO}_3)_2 \cdot 6\text{H}_2\text{O}$ and (0.03 M) Hexamethylenetetramine (HMT) [19] was prepared with triple distilled water. The solution was stirred for 5 min before heating. The substrates were lowered with seeded face down into the solution and the whole system was stirred constantly. The temperature was maintained at 90°C . The typical growth was done for 5–8 h in order to grow nanorods with lengths more than $1\ \mu\text{m}$. The alignment of the nanorods is in the growth direction and the extent of the orientation (which we call texture) depends on the time of growth. The texture is enhanced as the growth progresses in time. After the desired time of growth, the samples were taken out of solution and rinsed with de-ionized water and dried. The as-grown rods were not subjected to any further heat treatment and could be directly used for experiments.

2.3. Characterization methods used

The seed nanoparticles and the nanorods were characterized by X-ray diffraction (XRD), UV-Visible spectrometer, Scanning Electron Microscope (SEM, JEOL 12 kV) and Scanning Probe Microscope (SPM). We used an Autoprobe[®] CP –R SPM machine from Veeco Instruments Inc. TEM images and SAED (selective area electron diffraction pattern) was carried out in a JEOL machine and the voltage used was 200 kV.

3. Results and discussion

3.1. Seed nanoparticles

In Fig. 1 we show XRD data for nanoparticles as well as micron-sized powder of ZnO. The XRD pattern of the nanoparticles shows all the major peaks expected of wurtzite structure ZnO. TEM study of the nanoparticles

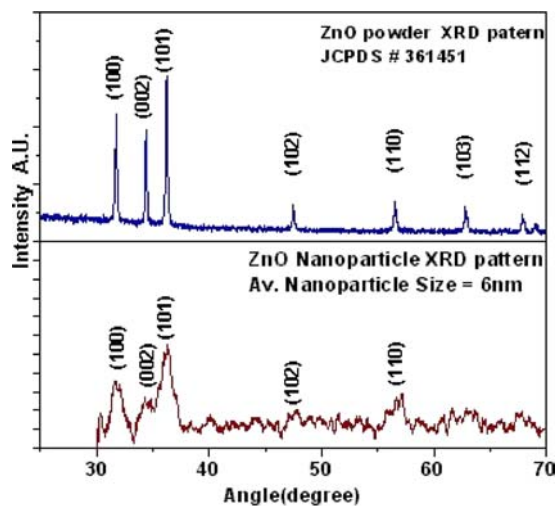


Figure 1 XRD pattern of the seed nanoparticles (lower trace) compared with ZnO powder (micron-size) prepared by standard ceramic methods.

also shows this average size and the high-resolution image shows that the particles are single nano-crystalline particles. From TEM, XRD and contact mode imaging of the seeded surface we found that the average particle size for the seed particle is around $\approx 5-6$ nm. The seeded surface has a typical particle density of $10^{11}-10^{12}/\text{cm}^2$.

3.2. Nanorods

In Fig. 2 we show XRD pattern of the nanorods grown in the solution as a function of growth time. The XRD lines correspond to Wurtzite structure with lattice spacing $c = 0.5206$ nm which matches with that reported for the bulk ZnO. It can be seen that the alignment of the nanorods along a certain growth direction start very early in the growth process. Within 2 h of initial growth the

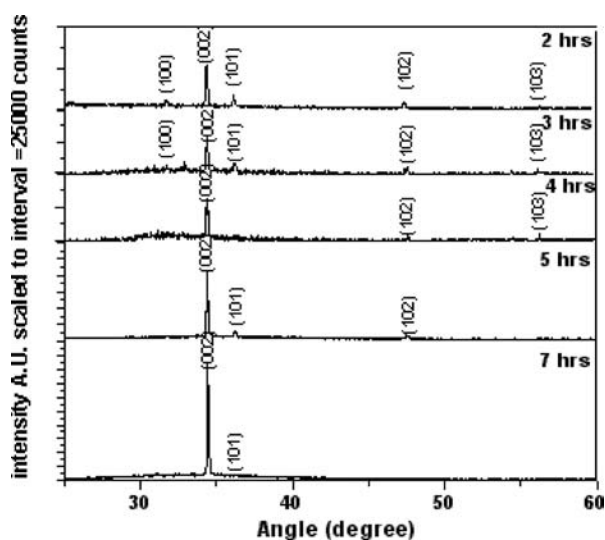
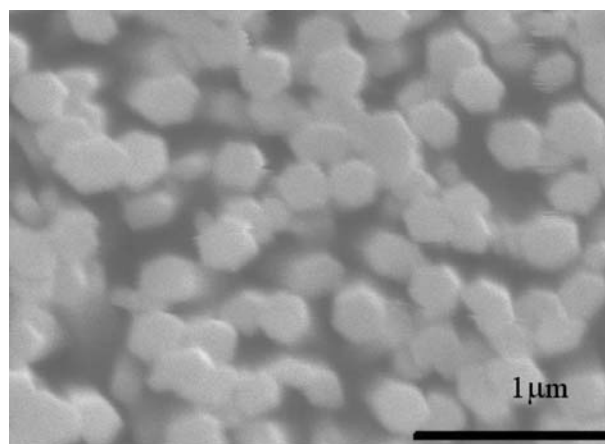


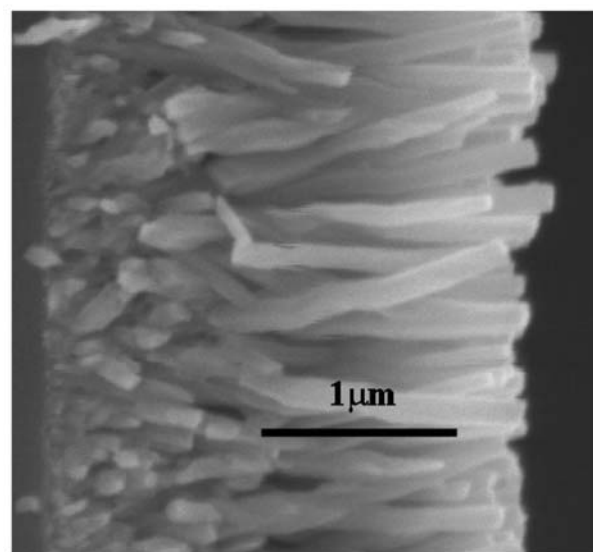
Figure 2 XRD pattern for ZnO nanorods grown onto seeded surface of Si as a function of growth time. The progressive alignment with growth time can be seen (the (002) reflection is only seen after sufficient time).

texture coefficient $R_{\text{texture}}(hkl)$ (defined as the ratio of intensity of a particular peak, with index hkl , to sum of intensities all major peaks) reaches more than 50% for (002) peak and as the growth proceeds the alignment along the (002) direction becomes more perfect and within 5 h of growth (for the given growth condition) reaches more than 80%. At the final stages of growth a texture coefficient for the (002) peak of about 90% is reached. We note that the initial seeded surface had random orientation much like a polycrystalline surface. This alignment of the nanorods along the (002) direction occurs during the growth process.

In Fig. 3 we show SEM images of aligned nanorods. The SEM images show the top view (Fig. 3a) as well as the side view (Fig. 3b). From the side view we can directly see the aligned array of the nanorods. The SEM image shows very clearly that the nanorods grow to nearly the same height and orientations. It can be seen that there are large number of very short rods with random growth orientation lying at



(a)



(b)

Figure 3 SEM images of the aligned ZnO nanorods on Si substrate at a magnification of $25,000\times$. (a) top view, (b) side view.

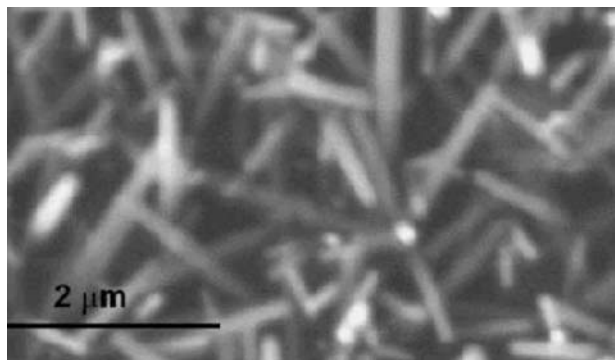


Figure 4 SEM images of the nanorods grown on a surface with no seeding.

the base near the seeded surface. Presumably this may be the misaligned rods that cannot grow to sufficiently large size. As a result the texture becomes more perfect as the growth proceeds as revealed by the XRD. The role of the seeding in the growth process can be appreciated when the similar process for growth is carried out on the Si substrate without the seeding particles. This can be seen in the SEM images of Fig. 4. The figure shows the growth of nanorods is completely random and most of them are lying on the surface. Thus seeding is absolutely essential for aligned growth. The seeding makes the aligned nanorods growth more or less independent of the substrate used as similar aligned growth has been found on a number of different types of substrates including amorphous and crystalline substrate materials. We observe that the initial seeded surface has a particle density of $\sim 10^{11}$ – $10^{12}/\text{cm}^2$. After the growth the nanorods the density is $\sim 10^9/\text{cm}^2$. Thus on the average one in about 100–1000 of the seeds gives rise to nanorods that are aligned and grow to a sufficient size.

The distribution of the widths of the nanorods is unimodal as can be seen from the distribution histogram obtained from the SEM data and shown in Fig. 5, which is a typical distribution after a 3 h growth. The distribution fits a log-normal form of distribution.

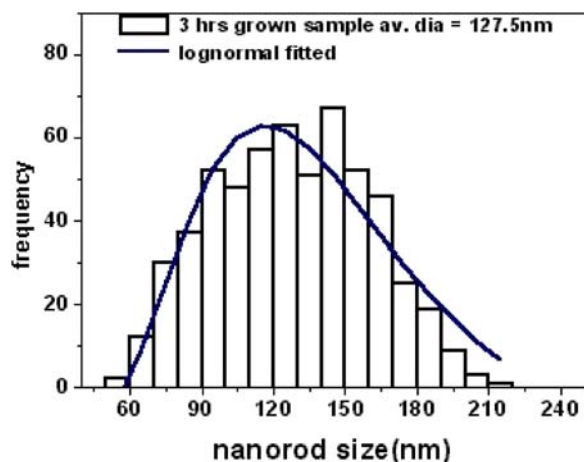


Figure 5 Width distribution of ZnO nanorods for 3 hrs-grown samples. The fit shows a log normal distribution.

The TEM images of the typical nanorods and also the SAED pattern are shown in Fig. 6. The TEM images were taken by scraping the rods from substrate and dispersing in acetone. The images are for rods grown for about 3 h. The SAED pattern matches with that of a hexagonal Wurtzite structure.

The contact mode AFM images of the nanorods are shown in Fig. 7. The scans were taken with a normal contact force of ≈ 8 nN and with a cantilever of spring constant $k \approx 0.16$ N/m. The data are shown for the samples with longest growth time and the average width of the rod reaches ≈ 230 – 250 nm. The image in Fig. 7a (scan size $10 \mu\text{m} \times 10 \mu\text{m}$) was taken with a tilt of the samples so that the growth pattern is visible. It can be seen that the growth is rather dense and uniform with occasional gaps/voids in the growth pattern. These gaps/voids generally occur where there are fewer seed particles. A small area scan ($1 \mu\text{m} \times 1 \mu\text{m}$) is given in Fig. 7b where one can clearly see the hexagonal cross-section of the nanorods grown. A close inspection of the data shows that along the nanorod walls there are clear growth patterns which presumably arise from crystallographic planes as the crystal grows. The clear growth spiral pattern on the tips of the nanorods can be seen in Lateral Force Microscopy (LFM) images of the nanorods. An example of this is shown in Fig. 8. The growth spirals are close to hexagons. These growth patterns are typical of growth spirals that occur in growing crystals. The observation of the growth spiral is important because it implies that the nucleation occurs at the screw dislocation on the growing surface. There is no random nucleation where the nanorods grow. This is needed for such an aligned growth process, as random nucleation will lead to growth along any of the growth directions. In fact it is the slow solution growth that is needed for such a well-defined growth process and gives rise to good quality materials.

The roughness of the ends of the nanorods becomes important for various applications like optical applications. From line scan on the AFM images of the ends of the nanorods we find that the rms roughness of the order of ~ 5.5 nm. An example of the line scan on a single nanorod is shown in 7c. A correlation of LFM and AFM (topographic data) shows that roughness is a result of growth spirals. For a crystal growth of this type, the presence of such spirals cannot be avoided. The c -axis parameter for the ZnO is ~ 0.5206 nm. Thus the rms roughness is ~ 10 lattice spacing, which is somewhat larger than what is expected from a growth in solution.

The quality of the material grown can be seen from its band gap as evaluated from its UV-Visible spectra. The gap value has been evaluated from the UV-Visible spectra shown in Fig. 9. We observe a typical value of the gap at ≈ 3.25 eV for the nanorods grown.

3.3. The time dependence of growth

The growth of the nanorods has a distinct dependence on the time of growth. The growth of the length as a

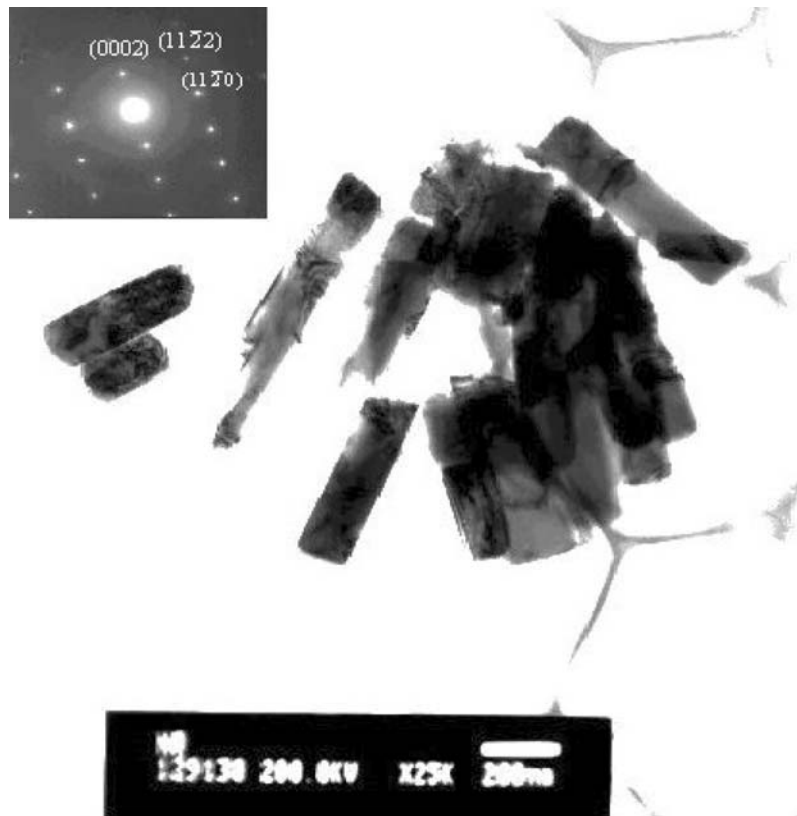


Figure 6 TEM image of the typical ZnO nanorods. The inset shows SAED pattern of a single nanorod.

function of time is shown in Fig. 10. It is representative of the growth process and has been obtained repeatedly in a number of growth experiments. When the growth conditions and parameters like temperature and concentration change, the curves qualitatively remain the same but quantitative changes occur. The width and length measurements were performed on the SEM data. The lengths and widths are distributed and the average length at each growth time was obtained from the distribution. Generally we find that while parameters are kept the same, the run to run variation is approximately $\pm 15\%$ as shown in the figure.

In the same graph, we also show the growth of the average width and texture coefficient for the (002) orientation and aspect ratio (\equiv length/width) as a function of time. We find that a good alignment (texture coefficient in excess of 50%) is generally obtained within 4 h of growth when the width is $\sim 140\text{--}150$ nm and the length is ~ 1 μm . Beyond that the texture coefficient grows slowly and length and width grows steadily, reaching a length of ~ 1.6 μm and width of ≈ 230 nm after 7 h of growth. These numbers may vary somewhat from different batches of growth but within $\pm 15\%$ they are reproducible. The texture coefficient in the initial stages may show some variability from batch to batch but the ultimate value $\sim 90\%$ is reproducibly achieved.

Comparison with previous growth studies shows that the nanorods obtained by us are of similar size and length, although the aspect ratio (length/width) of ≈ 7 is some-

what smaller than $\approx 8\text{--}10$ obtained by previous authors [15, 17]. However, as mentioned before, the dense seeding of the substrate (possibly due to smaller particle size used) led to much better orientation in the samples grown by us. We could achieve texture coefficients of more than 50% at early stages of growth and $\geq 90\%$ in the final stages (≥ 7 h) of growth. This may be compared with texture coefficient of 40–50% reported before [15, 16].

We note that the growth of the nanorods is very much dependent on seeding of the surface. As we have seen before in the absence of the seeding the nanorods grow from solution but they grow randomly as can be seen from the SEM shown in Fig. 4. The seeds presumably make the crystals grow in the fast growth direction, which is along the c -axis (001). From Fig. 10 we can see that there are two distinct growth phases when the growth starts from the seeded surface. This can be clearly seen in the growth curve for the length and the width. This is also seen in the growth of the texture. The first phase lasting till 4 h and the next phase beyond that. The texture also grows rapidly initially and then this is followed by a slow growth in the texture. It is suggested that the first regime of growth belong to an early random growth along the fast growth axis of the nanorods (anchored to the seeds). This random growth is then followed by an aligned growth. The alignment can arise from space constraints imposed on the growing rods due to dense packing of the seeds. The rods with alignments that are not along the normal to the substrate cannot grow due to

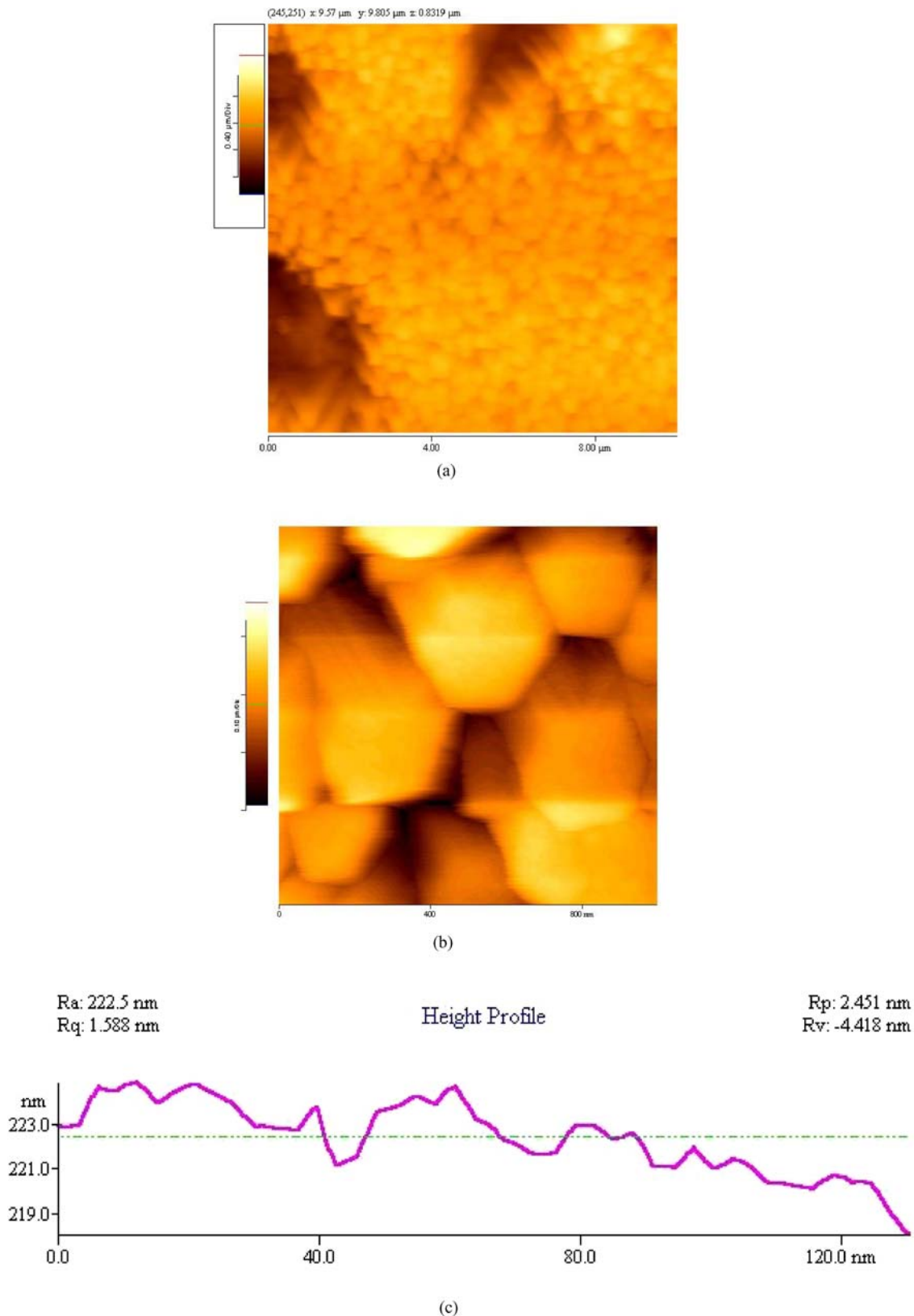


Figure 7 Contact mode Topographic image of ZnO nanorods. Scan size (a) $10\ \mu\text{m} \times 10\ \mu\text{m}$, (b) $1\ \mu\text{m} \times 1\ \mu\text{m}$, (c) Line scan on a typical nanorod tip.

confinement. The SEM images in Fig. 3b clearly show these misaligned rods with truncated growth lying on the substrate. Thus in the early stage, the texture coefficient grows and then after certain growth time it approaches

near saturation although the nanorods grow in length and width.

The time dependence of the growth process of length and width is not linear. In the first part of the growth

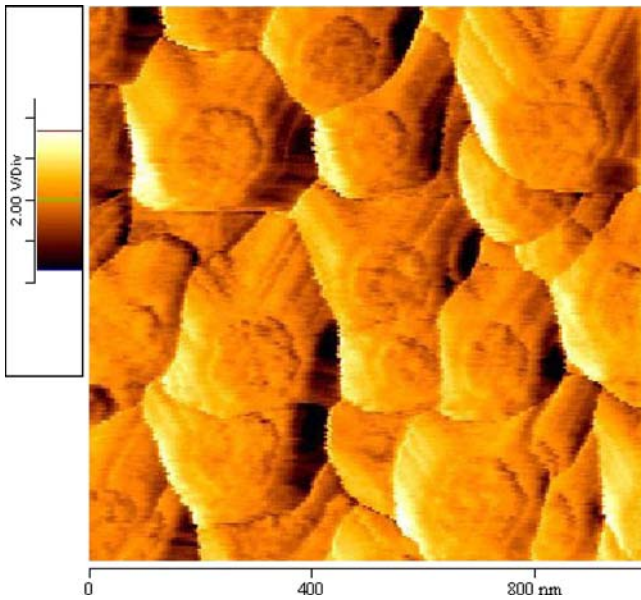


Figure 8 Lateral Force Microscopy (LFM) image of the tips of ZnO nanorods. Scan size is $1 \mu\text{m} \times 1 \mu\text{m}$.

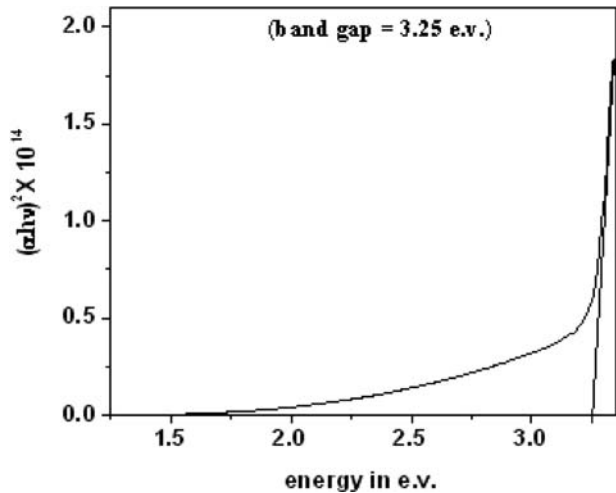


Figure 9 Band Gap of ZnO from UV-VIS data.

process (time < 4 h), both length and width grow almost at the same rate and time dependence $\propto t^{1/2}$, which one should expect from simple diffusion limited growth. Interestingly in this range we find the aspect ratio remains rather constant at ~ 7.5 (see Fig. 10). At the changeover stage there is a drop in aspect ratio and the texture also shows a dip (shown by an arrow in Fig. 10). Beyond that the aspect ratio again grows. In this range the length grows as $\propto t$ while width shows a sub-linear growth. As a result the aspect ratio is not constant and increases with time. At this stage of growth, it is the space constraint that severely limits the lateral growth of nanorods leading to sub-linear time dependence for growth of the width.

The data presented here clearly establishes that the nanorods grown are clearly aligned and compact and have structure and physical properties of a good quality single crystalline ZnO. The fact that the nanorods are anchored

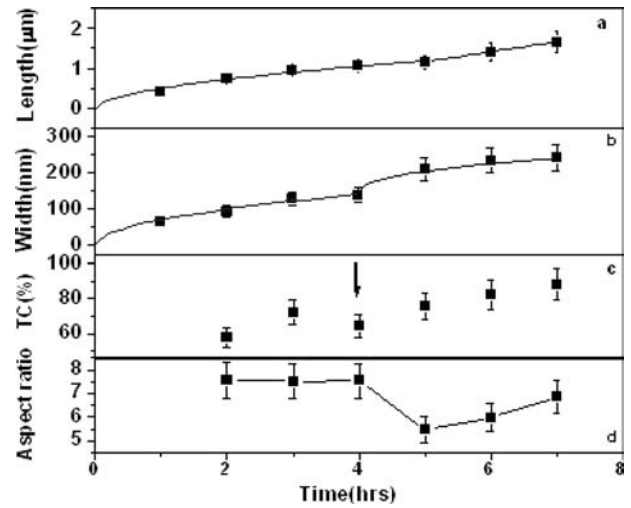


Figure 10 Dependence of (a) average length (b) average width (c) texture coefficient of (002) line (d) aspect ratio of the ZnO nanorods on growth time.

to a substrate makes the handling of the array easy. We find that the growth process completely covers the substrate with more or less uniform coverage. Thus the low temperature solution based route gives us a method to grow large area arrays of ZnO nanorods of good quality.

4. Conclusion

We have grown aligned ZnO nanorods (from seeds of pre-grown ZnO nanoparticles) by a low temperature ($< 100^\circ\text{C}$) solution growth method on Si surface. The method however is sufficiently general and can be grown on any smooth surface and it is amenable to large area growth. These aligned nanorods ($\sim 90\%$) were characterized by XRD, SEM, TEM and AFM and UV-Visible spectrometer and found to be good quality single crystals with adequate mechanical strength. These rods have potential application in devices where alignment and surface to volume ratio are predominant figures of merit.

Acknowledgment

Authors want to thank Dr. K. Shantha Shankar for useful discussions and initial work in this growth program. RC wants to thank Dr. V. B. Shenoy for useful discussions, Ms. L. K. Brar and Mr. T. P. Sai for their useful tips and help in SPM characterization and Mr. Suresh for TEM images. AKR wants to thank DST, Government of India for a sponsored project under Nanoscience and Technology Initiative.

References

1. D. G. THOMAS, *J. Phys. Chem. Solids* **15** (1960) 86.
2. M. H. HUANG, S. MAO, H. FEICK, H. YAN, Y. WU, H. KIND, E. WEBER, R. RUSSO and P. YANG, *Science* **292** (2001) 1897.
3. M. BENDER, E. GAGAOUKAKIS, E. DOULOFAKIS, E. NATSAKOU, N. KATSARAKIS, V. CIMALLA, G.

- KIRIAKIDIS, E. FORTUNATO, P. NUNES, A. MARQUES, and R. MARTINS, *Thin Solid Films* **418** (2002) 45.
4. S. MANIV and A. ZANGVIL, *J. Appl. Phys.* **49** (1978) 2787.
 5. T. YAMAMOTO, T. SHIOSAKI, A. KAWABATA, *J. Appl. Phys.* **51** (1980) 3113.
 6. M. H. HUANG, Y. WU, H. FEICK, N. TRAN, E. WEBER, and P. YANG, *Adv. Mater.* **13** (2001) 113.
 7. C. XU, G. XU, Y. LIU and G. WANG, *Solid State Commun.* **122** (2002) 175.
 8. J. ZHANG, S. LINGDONG, L. CHUNSHENG and Y. CHUNHUA, *Chem. Commun.* **262** (2002) 262.
 9. Y. W. WANG, L. D. ZHANG, C. Z. WANG, X. S. PENG, Z. Q. CHU and C. H. LIANG, *J. Cryst. Growth.* **234** (2002) 171.
 10. J. Q. HU, Q. LI, N. B. WONG, C. S. LEE and S. T. LEE, *Chem. Mater.* **14** (2002) 1216.
 11. Y. W. ZHU, H. Z. ZHANG, X. C. SUN, S. Q. FENG, J. XU, Q. ZHAO, R. M. WANG and D. P. YU, *Appl. Phys. Lett.* **83** (2003) 144.
 12. W. PARK, D. H. KIM, S. W. JUNG, and G. C. YI, *Appl. Phys. Lett.* **80** (2002) 4232.
 13. S. C. LIU and J. J. WU, *J. Mater. Chem.* **10** (2002) 3125.
 14. Y. LI, G. S. CHENG and L. D. ZHANG, *J. Mater. Res.* **15** (2000) 2305.
 15. L. VAYSSIERES, K. KEIS, A. HAGFELDT and S. E. LINDQUIST, *J. Phys. Chem. B* **105**(17) (2001) 3350.
 16. Z. R. TIAN, J. A. VOIGT, J. LIU, B. MCKENZIE, M. J. MCDERMOTT, M. A. RODRIGUEZ, H. KONISHI, and H. XU, *Nature Mater.* **2** (2003) 821.
 17. L. E. GREENE, M. LAW, J. GOLDBERGER, F. KIM, J. C. JOHNSON, Y. ZHANG, R. J. SAYKALLY and P. YANG, *Angew. Chem. Int. Ed.* **42** (2003) 3031.
 18. C. PACHOLSKI, A. KORNOWSKI, and H. WELLER, *Angew. Chem.* **114** (2002) 1234.
 19. R. TURGEMAN, O. GERSHEVITZ, O. PALCHIK, M. DEUTSCH, B. M. OCKO, A. GEDANKEN and C. N. SUKENIK, *Crystal Growth Design* **4** (2004) 169.

*Received 10 June
and accepted 9 August 2005*